



Published in final edited form as:

*J Pediatr.* 2018 February ; 193: 54–61.e2. doi:10.1016/j.jpeds.2017.09.083.

## Altered Cerebral Perfusion in Preterm Infants Compared with Full-term Infants

Marine Bouyssi-Kobar, MS<sup>a,b</sup>, Jonathan Murnick, MD-PhD<sup>a</sup>, Marie Brossard-Racine, PhD<sup>c</sup>, Taeun Chang, MD<sup>d</sup>, Eman Mahdi, MD<sup>a</sup>, Marni Jacobs, PhD<sup>e</sup>, and Catherine Limperopoulos, PhD<sup>a</sup>

<sup>a</sup>The Developing Brain Research Laboratory, Department of Diagnostic Imaging and Radiology, Washington DC, USA

<sup>b</sup>Institute for Biomedical Sciences, George Washington University, Washington DC, USA

<sup>c</sup>Department of Pediatrics Neurology, Montreal Children's Hospital-McGill University Health Center, Montreal QC, Canada

<sup>d</sup>Department of Neurology, Children's Research Institute, Children's National Health System, Washington DC, USA

<sup>e</sup>Department of Epidemiology and Biostatistics, Children's Research Institute, Children's National Health System, Washington DC, USA

### Abstract

**Objectives**—To compare regional cortical cerebral blood flow (CBF) in very preterm infants at term-equivalent age (TEA) and healthy full-term newborns, and to examine the impact of clinical risk factors on CBF in the preterm cohort.

**Study design**—This prospective cross-sectional study included very preterm infants (gestational age (GA) at birth <32 weeks; birth weight <1500g) and healthy full-term controls. Using non-invasive 3T arterial spin labeling MRI, we quantified regional CBF in the cerebral cortex: sensorimotor/auditory/visual cortex, superior medial/dorsolateral prefrontal cortex, anterior/posterior cingulate cortex (ACC/PCC), insula, and lateral posterior parietal cortex; as well as in the brainstem, and deep gray matter. Analyses were performed controlling for sex, GA, and age at MRI.

**Results**—We studied 202 infants: 98 preterm and 104 full-term infants at TEA. Preterm infants demonstrated higher global CBF ( $\beta=9.03$ ;  $P<.0001$ ) and higher absolute regional CBF in all brain regions except the insula. Relative CBF in the insula, ACC and auditory cortex were significantly decreased in preterm infants compared with their full-term peers ( $p<0.0001$ ;  $p=0.026$ ;  $p=0.036$ ,

---

**Corresponding author:** Dr. Catherine Limperopoulos, Director, Developing Brain Research Laboratory, Department of Diagnostic Imaging and Radiology, Children's National Health System, 111 Michigan Ave NW, Washington DC 20010, USA, (climper@childrensnational.org); Phone: + 202-476-5293; Fax: + 202-476-6833.

**Publisher's Disclaimer:** This is a PDF file of an unedited manuscript that has been accepted for publication. As a service to our customers we are providing this early version of the manuscript. The manuscript will undergo copyediting, typesetting, and review of the resulting proof before it is published in its final citable form. Please note that during the production process errors may be discovered which could affect the content, and all legal disclaimers that apply to the journal pertain.

The authors declare no conflicts of interest.

respectively). Additionally, the presence of parenchymal brain injury correlated with lower global and regional CBF (insula, ACC, sensorimotor, auditory, and visual cortices) while the need for cardiac vasopressor support correlated with lower regional CBF in the insula and visual cortex.

**Conclusions**—Altered regional cortical CBF in very preterm infants at TEA may reflect early brain dysmaturation despite the absence of cerebral cortical injury. Furthermore, specific cerebral cortical areas may be vulnerable to early hemodynamic instability and parenchymal brain injury.

## Keywords

rain development; cerebral cortex; premature birth; cerebral blood-flow; magnetic resonance imaging; arterial spin labeling

---

Very preterm infants born before 32 weeks' gestational age (GA) are at risk for neurodevelopmental disorders.<sup>1</sup> Brain development consists of genetically determined and environmentally influenced biological processes<sup>2</sup> that might be altered following preterm birth.<sup>3</sup> Specifically, during the “ex-utero” third trimester of very preterm infants, synaptogenesis, axonal/dendritic outgrowth, myelination, and gyrification are rapidly occurring and represent a critical period of brain development.<sup>4</sup> Altered cerebral maturation despite the absence of structural brain injury is increasingly reported in very premature infants<sup>5,6</sup> with evidence of disturbances in cerebral cortical development<sup>7</sup> and relationships to adverse neurodevelopmental outcome.<sup>8,9</sup>

Cerebral blood flow (CBF) delivers oxygen and nutrients required for optimal brain maturation, and it is coupled with brain metabolism.<sup>10</sup> Computation of CBF using nuclear medicine techniques has provided great insights regarding cerebral maturation in neonates,<sup>11–14</sup> however, the use of ionizing radiation presents an important limitation.<sup>15</sup> Arterial spin labeling (ASL) is a non-invasive magnetic resonance imaging (MRI) technique, that enables CBF quantification without the need for a contrast agent. Instead, ASL-MRI uses the water in arterial blood as an endogenous tracer.<sup>16</sup>

The successful application of ASL-MRI in high-risk newborns facilitates the non-invasive assessment of brain maturation, injury, and repair through CBF quantification.<sup>20</sup> To date, no study has specifically focused on characterizing cerebral cortex CBF in very preterm infants at TEA despite the emerging evidence of impaired cerebral cortical maturation following preterm birth.<sup>24–26</sup> Therefore, we sought to examine the impact of preterm birth on regional cerebral cortical perfusion. We compared CBF in preterm infants at TEA (n=98) with normative CBF data acquired in a large sample of healthy full-term neonates (n=104). Additionally, we investigated clinical risk factors associated with preterm birth that could potentially influence cerebral perfusion.

## Methods

Infants were prospectively enrolled at Children's National Health System (Washington, DC) from June 2012 to December 2015.<sup>5</sup> Preterm infants were eligible if born before 32 weeks of gestation with a birth weight <1500 grams. Exclusion criteria included: chromosomal anomalies, dysmorphic features, congenital brain malformations, central nervous system

infection, metabolic disorders, severe brain injury (defined using brain scoring classification),<sup>27</sup> and residual active analgesic/sedative medications at the time of the MRI study. In the context of another observational study on fetal/newborn brain growth and development, healthy fetal/mother dyads with normal fetal sonography were enrolled as control participants.<sup>5</sup> Exclusion criteria included chromosomal abnormalities, multiple gestations, congenital infections, and maternal disease/drug use. All healthy control participants were born at full-term with uneventful deliveries and normal MRI brain scans. Both studies were approved by the Institutional Review Board and written informed consent was obtained from the parents at enrollment of each participant.

Demographics and clinical information collected are shown in Table I. In the preterm cohort, the clinical risk factors of interest recorded were: chorioamnionitis, moderate to severe bronchopulmonary dysplasia,<sup>28</sup> length of oxygen support, postnatal steroid treatment, sepsis (confirmed by positive blood culture), necrotizing enterocolitis, need for cardiac vasopressor support, and patent ductus arteriosus ligation.

## MRI Acquisition and Image Analysis

Brain MRI sequences were performed on a 3-T Discovery MR750 scanner (GE Healthcare, Milwaukee, Wisconsin) for all participants. Infants were scanned under natural sleep. Proton density control images and perfusion weighted images were obtained with a 3D ASL sequence using pseudo-continuous labeling method, 3D FSE spiral readouts, and background suppression (echo/repetition time=11/4326 ms; voxel size=1.88×1.88×3 mm<sup>3</sup>; spiral acquisition= 512 samples by 8 arms; acquisition time=3 min). Pseudo-continuous ASL was used as it has a higher signal-to-noise ratio than conventional ASL.<sup>17-19</sup> Anatomical 3D T2-weighted CUBE images were also acquired (voxel size=0.63×0.63×1 mm<sup>3</sup>).

Clinical readings of all MRI studies were performed. An experienced pediatric neuroradiologist reviewed the preterm infant images and defined intraventricular hemorrhage severity<sup>29</sup> and brain injury severity.<sup>27</sup> Preterm infants were categorized into two groups based on the presence or absence of parenchymal brain injury.

The CBF map was computed in mL/100g/min from the ASL sequence with Functool software (GE Healthcare, Milwaukee, WI) using the general kinetic model:<sup>30</sup>

$$CBF = 6000 \times \lambda \times \frac{\left(1 - \exp\left(-\frac{ST}{T_{1t}}\right)\right) \times \exp\left(\frac{PLD}{T_{1b}}\right)}{2T_{1b} \times \left(1 - \exp\left(-\frac{LT}{T_{1b}}\right)\right) \times \varepsilon \times NEX_{PW}} \times \left(\frac{PW}{SF_{PW} \times PD}\right)$$

where the partition coefficient  $\lambda$  was set to 0.9; the saturation time (ST) was 2 s; the T1 of the cerebral gray matter (T<sub>1t</sub>) was set to 1.2 s; the longitudinal relaxation time of the blood (T<sub>1b</sub>) appropriate for MRI studies at TEA was assumed to be 1.85 s;<sup>31</sup> the post labeling delay (PLD) was set to 1025 ms; the labeling duration (LT) was 1.5 s; the overall efficiency ( $\varepsilon$ ) was 0.6, it was a combination of the inversion efficiency (80%) and the background suppression efficiency (75%); PW was the perfusion weighted image; the scaling factor of

the perfusion weighted ( $SF_{pw}$ ) was 32, the partial saturation of the reference image (PD) was 50%, and the number of excitation for the PW image ( $NEX_{pw}$ ) was 3.

Although background suppression was used to reduce motion artifact, some CBF maps were corrupted by severe head motion characterized by high signal intensity spiral.<sup>32</sup> Whenever possible, the motion corrupted ASL sequence was re-run during the scanning session (8 preterm/ 5 full-term infants); otherwise, CBF maps degraded by motion were discarded. After this quality check, the remaining CBF maps were manually skull-stripped before computing the global CBF (CBF map average). The high resolution T2-weighted image was then co-registered to its corresponding CBF map using affine registration.<sup>33</sup> Manual regions of interest (ROIs) were placed on the CBF map using the aligned anatomical image as guidance. Our cerebral cortical ROIs incorporated areas involved in primary motor/sensory tasks: the sensorimotor cortex (central sulcus), the auditory cortex (superior transverse gyrus), and the visual cortex (calcarine cortex); and cortical areas known to mediate higher cognitive processing: the superior medial and the dorsolateral prefrontal cortices, the anterior cingulate cortex (ACC), the posterior cingulate cortex, the insula, and the lateral posterior parietal cortex (Figure 1). Furthermore, we measured CBF in ROIs that are known to be the most metabolically active in newborns:<sup>34</sup> the deep GM including thalamus (pontine nucleus) and basal ganglia, and the brainstem (pons). The volume of each ROI was kept constant at 42.2 mm<sup>3</sup>. Intra-rater and inter-rater reliability were assessed via intraclass correlation coefficients on a randomly selected subset of 15 preterm/15 full-term infants. The intraclass correlation coefficients for intra-rater measurements ranged from 0.86 to 0.96 (median: 0.93) and for inter-rater measurements it ranged from 0.82 to 0.97 (median: 0.88).

## Statistical Analyses

Statistical analyses were performed using the Statistical Analysis Software version 9.3 (SAS Institute, Cary, NC). The effect of group (preterm versus full-term) on global CBF was analyzed with ANCOVA, adjusting for sex, GA and age at MRI. For regional CBF, paired t-tests revealed no clinically meaningful significant difference between left and right hemispheres for bilateral regions, thus hemispheric CBF values were averaged. Relative regional CBF was defined as the ratio of the ROI absolute CBF over the global CBF. To assess regional CBF between and within infants, we fitted linear mixed models using an unstructured covariance matrix structure within subjects; the choice of covariance matrix was guided by Akaike Information Criteria statistics.<sup>35</sup> The fixed effects were group, ROIs, sex, GA, age at MRI and the interaction between group and ROIs. Corrections for multiple comparisons were performed using Tukey-Kramer adjustment.

Within the preterm cohort, we used linear regression analysis to examine the relationship between global/regional CBF and each clinical risk factor individually controlling for sex, GA, and age at MRI. Of note, twelve preterm infants had low-grade intraventricular hemorrhage (grade I/II) on MRI findings; they were included in the “no parenchymal brain injury” group as there were no significant differences in global and regional CBF compared with the group with unremarkable anatomical MRI brain studies. A multiple regression analysis evaluated the combined effects of each of the clinical risk factors associated with differences in any global or regional CBF at  $p < 0.05$  (extended model). None of the

interactions between main effects were significant; consequently, they were not included in the extended model.

## Results

Of the 128 preterm infants scanned at TEA, 30 (23%) preterm infants were excluded: 9 (7%) infants had residual analgesic/sedative effects at the time of MRI, 13 (10%) had severe brain injury, 5 (3%) exceeded our TEA window (38 to 44 weeks of post-menstrual age [PMA]), and 3 (2%) had unusable data due to excessive motion. Of the 115 healthy full-term infants with ASL data, six (5%) were scanned after 44 weeks PMA and 5 (4%) presented with motion corrupted data and were excluded from the analyses. The clinical characteristics of the 202 infants studied (98 preterm infants/104 full-term controls) are summarized in Table 1. Preterm infants were scanned at a younger PMA compared with healthy full-term controls (40.12 versus 41.22 weeks, respectively).

The unadjusted average global CBF expressed in mL/100g/min was 19.21 (SD=4.2; range=9.4–29.7) in preterm infants and 13.38 (SD=4.29; range=8–21.3) in full-term controls. Preterm infants had significantly higher global CBF ( $\beta=9.03$ ; 95%CI= [5.73; 12.33];  $p<0.0001$ ). GA and age at MRI were positively associated with global CBF ( $\beta=1.01$ ; 95%CI= [0.6; 1.4];  $p<0.0001$ ; [ $\beta=0.12$ ; 95%CI= [0.06; 0.18];  $p<0.0001$ ; respectively); there was no association with sex ( $p=0.11$ ).

Regional absolute CBF significantly correlated with group status (preterm/full-term infants), ROIs, GA at birth, and age at MRI ( $p<0.001$ ); sex had no significant effect ( $p=0.39$ ). The interaction between group and ROIs was significant ( $p<0.0001$ ). The absolute CBF was significantly higher in preterm infants compared with healthy full-term control infants in all brain regions except the insula (Table 2.)

In the control infants, the brain areas with the highest relative CBF were the brainstem, insula, thalamus, and basal ganglia, respectively (Table 2). Within the cerebral cortex, the ACC and sensorimotor cortex had the highest relative CBF while the dorsolateral prefrontal cortex relative CBF was the lowest. When comparing relative CBF between groups, the significant fixed effects were group status, ROIs, and their interaction ( $p<0.05$ ). Specifically, the regional relative CBF in the insula, ACC and auditory cortex was significantly decreased in the preterm cohort (Table 2). Figure 2 (available at [www.jpeds.com](http://www.jpeds.com)) illustrates the regional CBF distribution per group status.

Among the clinical risk factors evaluated, the presence of parenchymal brain injury and the need for cardiac vasopressor support were associated with decreased global/regional CBF (Table 3). Parenchymal brain injury was associated with significantly decreased global CBF and decreased CBF in the insula, ACC, and sensorimotor/auditory/visual cortices (Figure 3; available at [www.jpeds.com](http://www.jpeds.com)); all these associations except the sensorimotor cortex remained significant in the extended model (Table 4; available at [www.jpeds.com](http://www.jpeds.com)). The need for cardiac vasopressor support was significantly associated with decreased regional CBF in the insula and visual cortex (Table 4).

## Discussion

In this prospective observational study, we demonstrated that global and regional CBF was altered in a large cohort of very preterm infants assessed at TEA compared with healthy full-term newborns. We found that relative CBF in the insula, ACC, and auditory cortex was lower in preterm infants. Within the preterm cohort, there was an association between parenchymal brain injury, cardiac vasopressor support and decreased regional CBF. Collectively, these results suggest altered functional brain maturation in very preterm infants by TEA.

Available data on cerebral perfusion in healthy full-term newborns are very limited<sup>21, 36, 37</sup> but necessary for establishing comparisons with high-risk neonatal populations. Although CBF measurements using positron emission tomography have traditionally served as reference values (mean global CBF between 18 to 24 mL/100g/min),<sup>13, 38, 39</sup> the sample population studied was small (N<10) and was comprised of infants who suffered perinatal asphyxia. In a healthy cohort of full-term infants, global CBF was previously estimated to be between 11 to 23 mL/100g/min.<sup>21, 36, 37</sup> Our normative CBF data are in keeping with these findings and suggest an underestimation of CBF with ASL-MRI compared with positron emission tomography. Specifically, our absolute CBF values are likely underestimated due to the use of a very short post labeling delay time. Nonetheless, our results provide important and currently limited data on brain perfusion in a large cohort of healthy full-term newborns.

Developmental trajectories of regional CBF reflect brain maturation,<sup>14</sup> with the highest CBF reported in the brainstem and deep gray matter in newborns.<sup>12, 22, 40, 41</sup> We found that the insula was one of the most perfused cerebral cortical areas. This has not been previously described, possibly due to the lower resolution of images from nuclear medicine techniques that make it difficult to distinguish the deep gray structures from the insula. In our study, the sensorimotor cortex, and the ACC had higher CBF than other cerebral cortical areas which corresponds to their previously reported higher glucose metabolic rate.<sup>34</sup> Analogous to other studies,<sup>11, 22</sup> the lateral frontal GM demonstrated low perfusion at TEA. Taken together, our findings highlight the early development of the insula, sensorimotor cortex and ACC.

Quantitative data on CBF in very preterm infants at TEA are scarce.<sup>21–23, 36</sup> We report higher global and regional CBF in very preterm infants at TEA compared with full-term controls, corroborating the results of Miranda et al.<sup>21</sup> The mechanisms underlying the elevated absolute CBF in preterm infants are complex, and likely multifactorial. One plausible hypothesis is that impaired parasympathetic control can lead to increased CBF.<sup>42, 43</sup> Another hypothesis would be that regional cerebral metabolic requirements are modified due to extra-uterine environment and associated external stimuli responsible for experience-dependent cortical development.<sup>44</sup> Finally, an association between dendritic arborization or synaptogenesis and elevated local CBF has also been suggested.<sup>23</sup>

Our study examined relative regional cerebral cortical perfusion and found a significant decrease in relative CBF in the insula, ACC, and auditory cortex in very preterm infants compared with full-term infants. The insula is one of the first cerebral cortical areas to develop and differentiate between 13 and 28 weeks GA.<sup>45</sup> Likewise, the ACC is also among

the first cerebral cortical regions to mature.<sup>46</sup> Finally, the auditory cortex is functionally active from 28 weeks GA when activity-dependent processes start shaping auditory cortical organization.<sup>47</sup> We postulate that decreased relative cortical CBF may be related to unmet increased metabolic requirements during early ex-utero third trimester exposure following preterm birth and may suggest specific regional susceptibility.

The insula of growth-restricted fetuses previously has been shown to exhibit alterations in biometric, volumetric, and microstructural organization compared with age-matched control fetuses, suggesting that the insula may be vulnerable when exposed to a hostile environment in the third trimester.<sup>48</sup> The insula is also the region reported to have the greatest disturbance in sulcal depth and cortical shape in preterm infants at TEA.<sup>7</sup> It is noteworthy that the insula and ACC are part of the salience network which is implicated in multiple neurodevelopmental disorders,<sup>49</sup> and compromised in adults born preterm.<sup>50</sup> Altered development of the insula and ACC may represent early biomarkers that may assist in identifying preterm infants at higher risk for long-term neurodevelopmental impairments.

The maturation of the auditory cortex depends heavily on exogenous auditory stimulation.<sup>47</sup> Consequently, early exposure to an atypical acoustic environment may alter development of the auditory network as demonstrated in animal studies.<sup>51, 52</sup> Preterm infants in the neonatal intensive care unit (NICU) are both deprived of maternal sounds (e.g., heart beat) and surrounded by noxious auditory stimuli that may negatively affect auditory system development.<sup>53</sup> The temporal cortex of preterm infants has been shown to exhibit cortical folding alterations<sup>7, 54</sup> and its decreased micro-structural organization has been associated with poorer language outcome.<sup>55</sup> Similarly, our results underscore a regional vulnerability of the developing auditory cortex in preterm infants. The influence of the NICU environment (private room vs open ward) has provided mixed outcomes;<sup>56, 57</sup> the balance between adverse acoustic noises and positive auditory stimulations (eg, meaningful language) appears critical to enhance auditory network development.<sup>53, 58</sup> Collectively, these data highlight the need for active monitoring of the different type of acoustic levels in the NICU in relationship to auditory cortex development.

It is well-established that prematurity-related white matter injury is associated with neuronal loss and gliosis in the cerebral cortical gray matter,<sup>59</sup> and decreased cortical volume.<sup>60</sup> However, the effect of preterm brain injury on CBF has not been previously investigated. We report that parenchymal brain injury is related to decreased global and regional CBF (insula, ACC, sensorimotor/auditory/visual cortex). These regions of interest are known to develop earlier than other cortical regions, with primary motor/sensory areas preceding the development of associative and prefrontal cortical areas.<sup>7, 61</sup> Consequently, early preterm brain injury may lead to dysmaturation in cortical areas actively developing over the third trimester, ex-utero.

Postnatal hypotension or its treatment with cardiac vasopressor medications were associated with lower perfusion in the insula and visual cortex. The timing of the high metabolic demands of the insula and visual cortex may overlap with prematurity-related hemodynamic instability, leading to region-specific alterations. Because we used a categorical variable for cardiac vasopressor support during infants' hospitalization, we cannot elucidate the

relationship between the length of treatment and cerebral cortical maturation, but it warrants future investigation. Previous studies have shown that cerebral oxygenation rather than hypotension alone is associated with neurodevelopmental outcome.<sup>62</sup> Even though ligation of a patent ductus arteriosus is associated with increased hemodynamic instability, we did not find an association with cerebral perfusion at TEA. Previous work has suggested that the duration of decreased cerebral oxygenation is a better predictor of cerebral growth impairment than ductal ligation.<sup>63</sup> Together these results emphasize that maintaining adequate cerebral oxygenation/perfusion following preterm birth is critical for normal brain development.

Although the MRI-ASL technique is not the gold standard for cerebral perfusion, it has been increasingly used in recent neonatal studies.<sup>20</sup> Non-invasive and free of ionizing radiation, CBF quantification using MRI-ASL provides insights into brain injury/repair mechanism<sup>37, 64–67</sup> and brain maturation<sup>21–23</sup> in high-risk neonatal populations. The use of pseudo-continuous ASL in the newborn population has provided sufficient signal-to-noise ratio, better image quality, and enabled the identification of cerebral structures.<sup>18, 19</sup> One major limitation of our study is the lack of optimized neonatal acquisition variables: we used a short post-labeling delay time and it has been demonstrated that higher post-labeling delay values should be used in neonatal population.<sup>68</sup> Although both populations were scanned with the same sequence variables allowing for comparisons, our absolute CBF values are likely underestimated and caution should be used when extrapolating from our data. Furthermore, the use of a generic  $T_{1b}$  instead of a subject-specific  $T_{1b}$  is a limitation of our study; however, we selected a neonatal PMA appropriate  $T_{1b}$  that is closely related to the population average at TEA.<sup>31</sup> The ROIs approach is also a limitation of our study as it is rater-dependent, however, it is important to note that we achieved good reliability measurements that are comparable with other studies.<sup>23, 37</sup> Regional segmentation through registration to a neonatal atlas may improve the reliability of the measurements in future studies. Moreover, accuracy of regional CBF values could be improved through correction of partial volume effect: tissue-specific masks from participants' segmentation of high-resolution anatomical images can be used to estimate brain tissue contribution within an ASL voxel.<sup>69</sup> Thus, the potential influence of very low neonatal white matter CBF value on gray matter would be accounted for. Another limitation is the cross-sectional design which does not permit intra-subject CBF assessment. Future studies using longitudinal analyses would allow for prospective characterization of cerebral maturation following preterm birth. Finally, the predictive value of these early alterations of regional CBF on neurodevelopmental outcome in preterm infants is unknown and currently under investigation.

Despite these limitations, our study provides new information about cerebral cortical perfusion, including the regional-specific vulnerability of the insula, ACC, and auditory cortex following preterm birth, and a negative effect of parenchymal brain injury and cardiac vasopressor support on regional CBF in very preterm infants at TEA.



## Acknowledgments

We thank all the families that participated in this study. We thank Nickie Andescavage, MD, for her critical clinical feedback and Ms. Caitlyn Loucas, MS, for her assistance in recruitment.

Supported by the Canadian Institutes of Health Research (MOP-81116), the SickKids Foundation (XG 06-069), and the National Institutes of Health (R01 HL116585-01). M.B.K. is a PhD student in the Molecular Medicine Program of the Institute for Biomedical Sciences at the George Washington University. This work is from a dissertation to be presented to the above program in partial fulfillment of the requirements for the PhD degree.

## Abbreviations

<b>ACC</b>	Anterior cingulate cortex
<b>ASL</b>	Arterial spin labeling
<b>CBF</b>	Cerebral blood flow
<b>GA</b>	Gestational age
<b>NICU</b>	Neonatal intensive care unit
<b>PMA</b>	Post-menstrual age
<b>ROI</b>	Region of interest
<b>TEA</b>	Term-equivalent age

## References

1. Blencowe H, Lee AC, Cousens S, Bahalim A, Narwal R, Zhong N, et al. Preterm birth– associated neurodevelopmental impairment estimates at regional and global levels for 2010. *Pediatric Research*. 2013; 74:17–34. [PubMed: 24366461]
2. Silbereis JC, Pochareddy S, Zhu Y, Li M, Šestan N. The Cellular and Molecular Landscapes of the Developing Human Central Nervous System. *Neuron*. 2016; 89:248–68. [PubMed: 26796689]
3. Bennet L, Van Den Heuvel L, M Dean J, Drury P, Wassink G, Jan Gunn A. Neural plasticity and the Kennard principle: does it work for the preterm brain? *Clin Exp Pharmacol Physiol*. 2013; 40:774–84. [PubMed: 23735123]
4. Kostovi I, Jovanov-Milošević N. The development of cerebral connections during the first 20–45 weeks' gestation. *Semin Fetal and Neonatal Med*. 2006; 11:415–22. [PubMed: 16962836]
5. Bouyssi-Kobar M, Plessis Du AJ, McCarter R, Brossard-Racine M, Murnick J, Tinkleman L, et al. Third Trimester Brain Growth in Preterm Infants Compared With In Utero Healthy Fetuses. *Pediatrics*. 2016; 138:e20161640–0. [PubMed: 27940782]
6. Padilla N, Alexandrou G, Blennow M, Lagercrantz H, Aden U. Brain Growth Gains and Losses in Extremely Preterm Infants at Term. *Cereb Cortex*. 2015; 25:1897–905. [PubMed: 24488941]
7. Engelhardt E, Inder TE, Alexopoulos D, Dierker DL, Hill J, Van Essen D, et al. Regional impairments of cortical folding in premature infants. *Ann Neurol*. 2014; 77:154–62. [PubMed: 25425403]
8. Rathbone R, Counsell SJ, Kapellou O, Dyet L, Kennea N, Hajnal J, et al. Perinatal cortical growth and childhood neurocognitive abilities. *Neurology*. 2011; 77:1510–7. [PubMed: 21998316]
9. Kersbergen KJ, Leroy F, Išgum I, Groenendaal F, de Vries LS, Claessens NHP, et al. Relation between clinical risk factors, early cortical changes, and neurodevelopmental outcome in preterm infants. 2016:1–40.
10. Volpe, JJ. *Neurology of the newborn*. 4. Philadelphia: 2001.

11. Børch K, Greisen G. Blood Flow Distribution in the Normal Human Preterm Brain. *Pediatric Research*. 1998; 43:28–33. [PubMed: 9432109]
12. Tokumaru AM, Barkovich AJ, O'uchi T, Matsuo T, Kusano S. The evolution of cerebral blood flow in the developing brain: evaluation with iodine-123 iodoamphetamine SPECT and correlation with MR imaging. *AJNR Am J Neuroradiol*. 1999; 20:845–52. [PubMed: 10369355]
13. Altman DI, Powers WJ, Perlman JM, Herscovitch P, Volpe SL, Volpe JJ. Cerebral blood flow requirement for brain viability in newborn infants is lower than in adults. *Ann Neurol*. 1988; 24:218–26. [PubMed: 3263081]
14. Chiron C, Raynaud C, Mazière B, Zilbovicius M, Laflamme L, Masure MC, et al. Changes in regional cerebral blood flow during brain maturation in children and adolescents. *J Nucl Med*. 1992; 33:696–703. [PubMed: 1569478]
15. Proisy M, Mtra S, Uria-Avellana C, Sokolska M, Robertson NJ, Le Jeune F, et al. Brain Perfusion Imaging in Neonates: An Overview. *AJNR Am J Neuroradiol*. 2016; 37:1766–73.
16. Detre JA, Leigh JS, Williams DS, Koretsky AP. Perfusion imaging. *Magn Reson Med*. 1992; 23:37–45. [PubMed: 1734182]
17. Avants BB, Duda JT, Kilroy E, Krasileva K, Jann K, Kandel BT, et al. The pediatric template of brain perfusion. *Sci Data*. 2015; 2:150003–17. [PubMed: 25977810]
18. Boudes E, Gilbert G, Leppert IR, Tan X, Pike GB, Saint-Martin C, et al. Measurement of brain perfusion in newborns: Pulsed arterial spin labeling (PASL) versus pseudo-continuous arterial spin labeling (pCASL). *Neuroimage Clin*. 2014; 6:126–33. [PubMed: 25379424]
19. Goff DA, Buckley EM, Durduran T, Wang J, Licht DJ. Noninvasive Cerebral Perfusion Imaging in High-Risk Neonates. *Sem Perinatol*. 2010; 34:46–56.
20. Wintermark P. Injury and repair in perinatal brain injury\_ Insights from non-invasive MR perfusion imaging. *Sem Perinatol*. 2015; 39:124–9.
21. Miranda MJ, Olofsson K, Sidaros K. Noninvasive Measurements of Regional Cerebral Perfusion in Preterm and Term Neonates by Magnetic Resonance Arterial Spin Labeling. *Pediatric Research*. 2006; 60:359–63. [PubMed: 16857776]
22. De Vis JB, Petersen ET, de Vries LS, Groenendaal F, Kersbergen KJ, Alderliesten T, et al. Regional changes in brain perfusion during brain maturation measured non-invasively with Arterial Spin Labeling MRI in neonates. *Eur Radiol*. 2013; 82:538–43.
23. Ouyang M, Liu P, Jeon T, Chalak L, Heyne R, Rollins NK, et al. Heterogeneous increases of regional cerebral blood flow during preterm brain development: Preliminary assessment with pseudo-continuous arterial spin labeled perfusion MRI. *NeuroImage*. 2017; 147:233–42. [PubMed: 27988320]
24. Dean JM, Bennet L, Back SA, McClendon E, Riddle A, Gunn AJ. What brakes the preterm brain? An arresting story. *Pediatric Research*. 2013; 75:227–33. [PubMed: 24336432]
25. Molnár Z, Rutherford M. Brain maturation after preterm birth. *Science Translational Medicine*. 2013; 5:168ps2–168ps2.
26. Back SA, Miller SP. Brain injury in premature neonates: A primary cerebral dysmaturation disorder? *Ann Neurol*. 2014; 75:469–86. [PubMed: 24615937]
27. Kidokoro H, Neil JJ, Inder TE. New MR Imaging Assessment Tool to Define Brain Abnormalities in Very Preterm Infants at Term. *AJNR Am J Neuroradiol*. 2013; 34:2208–14. [PubMed: 23620070]
28. Jobe AH, Bancalari E. Bronchopulmonary Dysplasia. *Am J Respir Crit Care Med*. 2001; 163:1723–9. [PubMed: 11401896]
29. Papile LA, Burstein J, Burstein R, Koffler H. Incidence and evolution of subependymal and intraventricular hemorrhage: a study of infants with birth weights less than 1,500 gm. *J Pediatr*. 1978; 92:529–34. [PubMed: 305471]
30. Buxton RB, Frank LR, Wong EC, Siewert B, Warach S, Edelman RR. A general kinetic model for quantitative perfusion imaging with arterial spin labeling. *Magn Reson Med*. 1998; 40:383–96. [PubMed: 9727941]
31. De Vis JB, Hendrikse J, Groenendaal F, de Vries LS, Kersbergen KJ, Benders MJNL, et al. Impact of neonate haematocrit variability on the longitudinal relaxation time of blood: Implications for arterial spin labelling MRI. *Neuroimage Clin*. 2014; 4:517–25. [PubMed: 24818078]

32. Amukotuwa SA, Yu C, Zaharchuk G. 3D Pseudocontinuous arterial spin labeling in routine clinical practice: A review of clinically significant artifacts. *J Magn Reson Imaging*. 2015; 43:11–27. [PubMed: 25857715]
33. Studholme C, Hill DLG, Hawkes DJ. An overlap invariant entropy measure of 3D medical image alignment. *Pattern Recognition*. 1999; 32:71–86.
34. Chugani HT. A critical period of brain development: studies of cerebral glucose utilization with PET. *Prev Med*. 1998; 27:184–8. [PubMed: 9578992]
35. Akaike H. Likelihood of a model and information criteria. *Journal of Econometrics*. 1981; 16:3–14.
36. Kehrer M, Krageloh-Mann I, Goelz R, Schöning M. The development of cerebral perfusion in healthy preterm and term neonates. *Neuropediatrics*. 2003; 34:281–6. [PubMed: 14681752]
37. Massaro AN, Bouyssi-Kobar M, Chang T, Vezina LG, Plessis du AJ, Limperopoulos C. Brain Perfusion in Encephalopathic Newborns after Therapeutic Hypothermia. *AJNR Am J Neuroradiol*. 2013; 34:1649–55. [PubMed: 23493898]
38. Rosenbaum JL, Almli CR, Yundt KD, Altman DI, Powers WJ. Higher neonatal cerebral blood flow correlates with worse childhood neurologic outcome. *Neurology*. 1997; 49:1035–41. [PubMed: 9339686]
39. Altman DI, Perlman JM, Volpe JJ, Powers WJ. Cerebral oxygen metabolism in newborns. *Pediatrics*. 1993; 92:99–104. [PubMed: 8516092]
40. Chugani HT, Phelps ME, Mazziotta JC. Positron emission tomography study of human brain functional development. *Ann Neurol*. 1987; 22:487–97. [PubMed: 3501693]
41. Shi Y, Zhao J-N, Liu L, Hu Z-X, Tang S-F, Chen L, et al. Changes of positron emission tomography in newborn infants at different gestational ages, and neonatal hypoxic-ischemic encephalopathy. *Pediatric Neurology*. 2012; 46:116–23. [PubMed: 22264707]
42. Brew N, Walker D, Wong FY. Cerebral vascular regulation and brain injury in preterm infants. *Am J Physiol Regul Integr Comp Physiol*. 2014; 306:R773–86. [PubMed: 24647591]
43. Fyfe KL, Yiallourou SR, Wong FY, Horne RSC. The development of cardiovascular and cerebral vascular control in preterm infants. *Sleep Med Rev*. 2014; 18:299–310. [PubMed: 23907095]
44. Jandó G, Mikó-Baráth E, Markó K, Hollódy K, Török B, Kovacs I. Early-onset binocularity in preterm infants reveals experience-dependent visual development in humans. *Proc Natl Acad Sci USA*. 2012; 109:11049–52. [PubMed: 22711824]
45. Afif A, Bouvier R, Buenerd A, Trouillas J, Mertens P. Development of the human fetal insular cortex: study of the gyration from 13 to 28 gestational weeks. *Brain Struct Funct*. 2007; 212:335–46. [PubMed: 17962979]
46. Slagle TA, Oliphant M, Gross SJ. Cingulate sulcus development in preterm infants. *Pediatric Research*. 1989; 26:598–602. [PubMed: 2689985]
47. Graven SN, Browne JV. Auditory Development in the Fetus and Infant. *Newborn and Infant Nursing Reviews*. 2008; 8:187–93.
48. Egaña-Ugrinovic G, Sanz-Cortes M, Figueras F, Couve-Perez C, Gratacós E. Fetal MRI insular cortical morphometry and its association with neurobehavior in late-onset small-for-gestational-age fetuses. *Ultrasound Obstet Gynecol*. 2014; 44:322–9. [PubMed: 24616027]
49. Uddin LQ. Salience processing and insular cortical function and dysfunction. *Nature Reviews Neuroscience*. 2015; 16:55–61. [PubMed: 25406711]
50. White TP, Symington I, Castellanos NP, Brittain PJ, Froudast-Walsh S, Nam KW, et al. Dysconnectivity of neurocognitive networks at rest in very-preterm born adults. *NeuroImage: Clinical*. 2014; 4:352–65. [PubMed: 24567907]
51. Chang EF, Merzenich MM. Environmental noise retards auditory cortical development. *Science*. 2003; 300:498–502. [PubMed: 12702879]
52. Sanes DH, Bao S. Tuning up the developing auditory CNS. *Current Opinion in Neurobiology*. 2009; 19:188–99. [PubMed: 19535241]
53. McMahon E, Wintermark P, Lahav A. Auditory brain development in premature infants: the importance of early experience. *Annals of the New York Academy of Sciences*. 2012; 1252:17–24. [PubMed: 22524335]

54. Zhang Y, Inder TE, Neil JJ, Dierker DL, Alexopoulos D, Anderson PJ, et al. Cortical structural abnormalities in very preterm children at 7 years of age. *NeuroImage*. 2015; 109:469–79. [PubMed: 25614973]
55. Aeby A, De Tiège X, Creuzil M, David P, Balériaux D, Van Overmeire B, et al. Language development at 2 years is correlated to brain microstructure in the left superior temporal gyrus at term equivalent age: a diffusion tensor imaging study. *NeuroImage*. 2013; 78:145–51. [PubMed: 23583746]
56. Vohr B, McGowan E, McKinley L, Tucker R, Keszler L, Alksninis B. Differential Effects of the Single-Family Room Neonatal Intensive Care Unit on 18- to 24-Month Bayley Scores of Preterm Infants. *J Pediatr*. 2017
57. Pineda RG, Neil J, Dierker D, Smyser CD, Wallendorf M, Kidokoro H, et al. Alterations in brain structure and neurodevelopmental outcome in preterm infants hospitalized in different neonatal intensive care unit environments. *J Pediatr*. 2014; 164:52–2. [PubMed: 24139564]
58. Pineda R, Durant P, Mathur A, Inder T, Wallendorf M, Schlaggar BL. Auditory Exposure in the Neonatal Intensive Care Unit: Room Type and Other Predictors. *J Pediatr*. 2017; 183:56–66. e3. [PubMed: 28189301]
59. Pierson CR, Folkerth RD, Billiards SS, Trachtenberg FL, Drinkwater ME, Volpe JJ, et al. Gray matter injury associated with periventricular leukomalacia in the premature infant. *Acta Neuropathol*. 2007; 114:619–31. [PubMed: 17912538]
60. Inder TE, Huppi PS, Warfield S, Kikinis R, Zientara GP, Barnes PD, et al. Periventricular white matter injury in the premature infant is followed by reduced cerebral cortical gray matter volume at term. *Ann Neurol*. 1999; 46:755–60. [PubMed: 10553993]
61. Huttenlocher PR, Dabholkar AS. Regional differences in synaptogenesis in human cerebral cortex. *J Comp Neurol*. 1997; 387:167–78. [PubMed: 9336221]
62. Alderliesten T, Lemmers PMA, van Haastert IC, de Vries LS, Bonestroo HJC, Baerts W, et al. Hypotension in preterm neonates: low blood pressure alone does not affect neurodevelopmental outcome. *J Pediatr*. 2014; 164:986–91. [PubMed: 24484771]
63. Lemmers PMA, Benders MJNL, D'Ascenzo R, Zethof J, Alderliesten T, Kersbergen KJ, et al. Patent Ductus Arteriosus and Brain Volume. *Pediatrics*. 2016; 137:peds.2015-3090-peds.2015-3090.
64. De Vis JB, Petersen ET, Kersbergen KJ, Alderliesten T, de Vries LS, van Bel F, et al. Evaluation of perinatal arterial ischemic stroke using noninvasive arterial spin labeling perfusion MRI. *Pediatric Research*. 2013; 74:307–13. [PubMed: 23797533]
65. Wintermark P, Lechpammer M, Warfield SK, Kosaras B, Takeoka M, Poduri A, et al. Perfusion Imaging of Focal Cortical Dysplasia Using Arterial Spin Labeling: Correlation With Histopathological Vascular Density. *J Child Neurol*. 2013; 28:1474–82. [PubMed: 23696629]
66. Nagaraj UD, Evangelou IE, Donofrio MT, Vezina LG, McCarter R, Plessis Du AJ, et al. Impaired Global and Regional Cerebral Perfusion in Newborns with Complex Congenital Heart Disease. *J Pediatr*. 2015; 167:1018–24. [PubMed: 26384435]
67. Watson CG, Dehaes M, Gagoski BA, Grant PE, Rivkin MJ. Arterial Spin Labeling Perfusion Magnetic Resonance Imaging Performed in Acute Perinatal Stroke Reveals Hyperperfusion Associated With Ischemic Injury. *Stroke*. 2016; 47:1514–9. [PubMed: 27143277]
68. Alsop DC, Detre JA, Golay X, Günther M, Hendrikse J, Hernandez-Garcia L, et al. Recommended implementation of arterial spin-labeled perfusion MRI for clinical applications: A consensus of the ISMRM perfusion study group and the European consortium for ASL in dementia. *Magn Reson Med*. 2014; 73:102–16. [PubMed: 24715426]
69. Asllani I, Borogovac A, Brown TR. Regression algorithm correcting for partial volume effects in arterial spin labeling MRI. *Magn Reson Med*. 2008; 60:1362–71. [PubMed: 18828149]

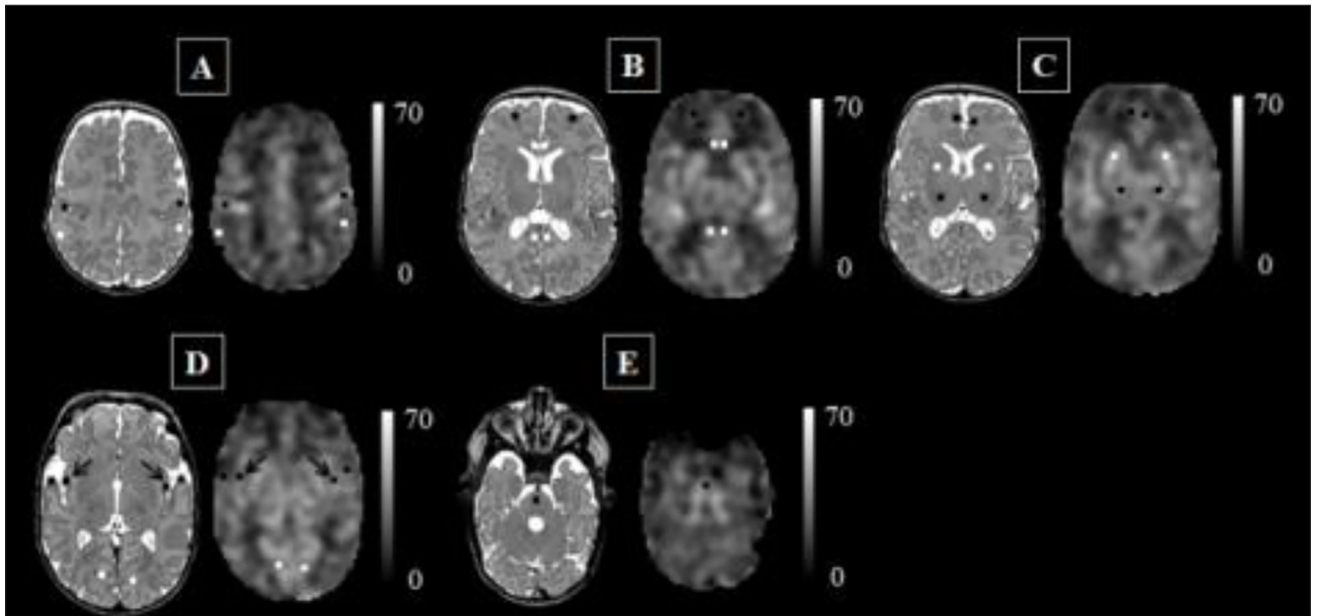


**Figure 1. Regions of interest, co-registered anatomical T2-weighted image and cerebral blood flow map**

Data from a preterm infant scanned at 43 weeks' post-menstrual age without evidence of parenchymal brain injury. Scale indicates cerebral blood flow unit mL/100g/min.

A = sensorimotor cortex (central sulcus) in black, lateral posterior parietal cortex in white; B = anterior cingulate cortex and posterior cingulate cortex in white, dorsolateral prefrontal cortex in black; C = superior medial prefrontal cortex in black, deep gray matter: basal ganglia in white, thalamus in black; D = insula in black (arrow), auditory cortex (superior transverse gyrus – temporal pole) in black, visual cortex (calcarine cortex) in white; E = brainstem.

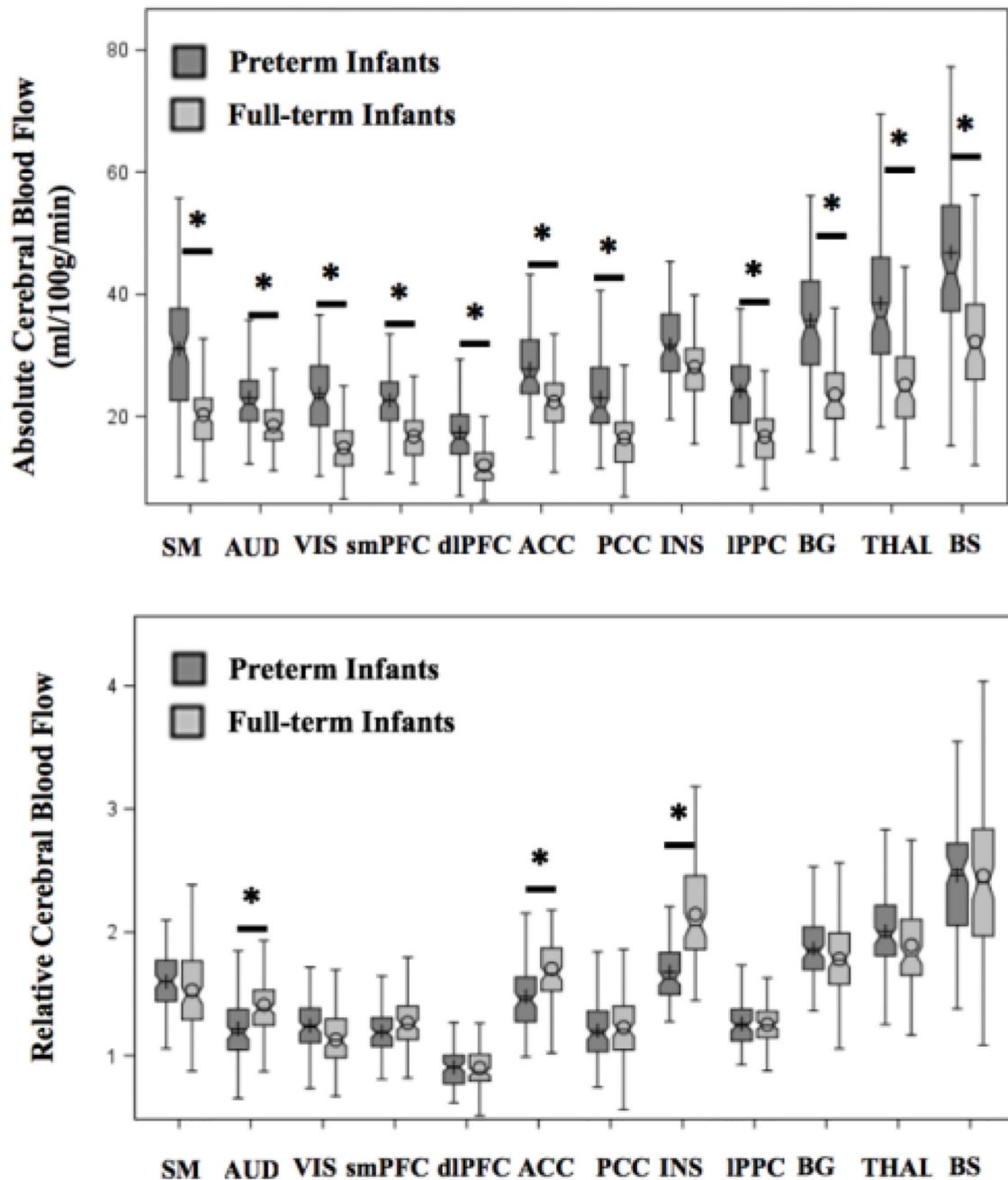


**Figure 2. Unadjusted boxplots of regional cerebral blood flow assessed in the preterm (n=98) and full-term (n=104) population at term-equivalent age**

\* Indicates the adjusted means between groups (preterm versus full-term infants) was significantly different ( $p < 0.05$ ) after adjustment for multiple comparisons using Tukey-Kramer, controlling for brain region, sex, gestational age at birth and day of life at MRI. ACC = anterior cingulate cortex; AUD = auditory cortex; BG = basal ganglia; BS = brainstem; dlPFC = dorsolateral prefrontal cortex; INS = insula; IPPC = lateral posterior parietal cortex; PCC = posterior cingulate cortex; SM = sensorimotor cortex; smPFC = superior medial prefrontal cortex; THAL = thalamus; VIS = visual cortex.

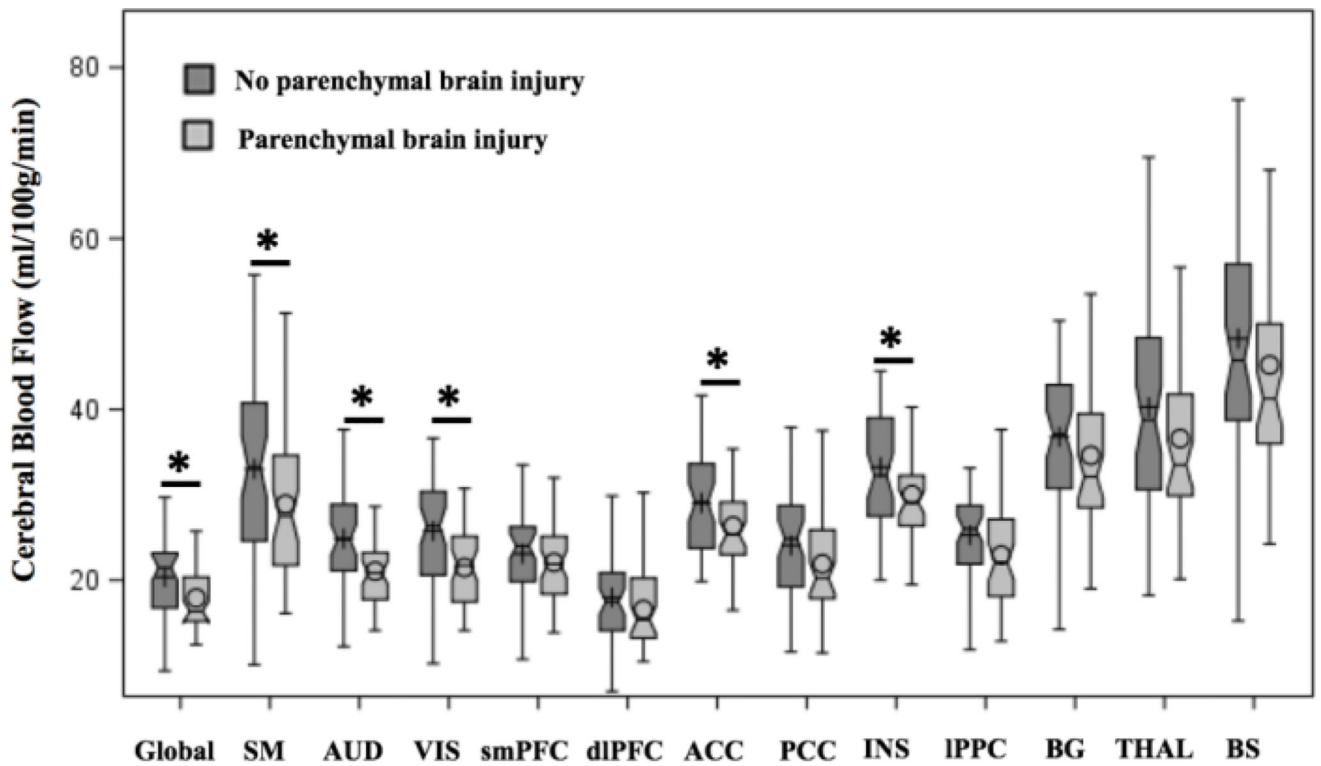


**Figure 3. Unadjusted boxplots of regional cerebral blood flow assessed in the preterm cohort according to the presence (n=47) /absence (n=51) of parenchymal brain injury**

\* Indicate the adjusted means between groups was significantly different ( $p < 0.05$ ) after adjustment for multiple comparisons using Tukey-Kramer, controlling for sex, gestational age at birth, and day of life at MRI.

ACC = anterior cingulate cortex; AUD = auditory cortex; BG = basal ganglia; BS = brainstem; dlPFC = dorsolateral prefrontal cortex; INS = insula; IPPC = lateral parietal cortex; PCC = posterior cingulate cortex; SM = sensorimotor cortex; smPFC = superior medial prefrontal cortex; THAL = thalamus; VIS = visual cortex.

**Table 1**

Clinical characteristics of the cohort (n=202)

	<b>Preterm Infants, n=98</b>	<b>Full-term Control Infants, n=104</b>	<b>P-value</b>
<b><u>Perinatal Characteristics</u></b>			
Birth GA, wk, mean $\pm$ SD	26.83 $\pm$ 2.58	39.58 $\pm$ 0.973	<0.0001
Birthweight, g, mean $\pm$ SD	886 $\pm$ 308	3353 $\pm$ 362	<0.0001
Small for gestational age, n (%)	12 (13)	9 (9)	0.4033
Male, n (%)	44 (45)	58 (56)	0.123
Native American; Hispanic; White Asian; Black; Multiethnic, n (%)	0; 22 (23); 12 (12) 58 (59); 6 (6)	2 (2); 9 (9); 31 (30) 10 (10); 48 (46); 4 (4)	<0.0001
Vaginal delivery, n (%)	37 (38)	74 (71)	<0.0001
Apgar score at 5 min, median [range]	7 [1–9]	9 [8–10]	<0.001
Maternal age, y, mean $\pm$ SD	27.79 $\pm$ 6.27	29.37 $\pm$ 6.66	0.0845
<b><u>MRI Characteristics</u></b>			
PMA at MRI, wk, mean $\pm$ SD	40.12 $\pm$ 1.39	41.22 $\pm$ 1.07	<0.0001
Age at MRI, d, mean $\pm$ SD	92.92 $\pm$ 20.14	11.42 $\pm$ 4.49	<0.0001
Head circumference at MRI, cm, mean $\pm$ SD	33.14 $\pm$ 1.97	35.62 $\pm$ 1.34 <sup>a</sup>	<0.0001
Supplemental oxygen at MRI, n (%)	27 (28)	na	na
Low-grade (I-II) IVH, n (%)	12 (12)	na	na
Parenchymal brain injury, n (%)	47 (48)	na	na
<b><u>Brain Abnormalities<sup>b</sup></u></b>			
Cystic white matter lesions, n (%)	5 (5)	na	na
Focal white matter signal abnormality, n (%)	20 (20)	na	na
Delayed myelination, n (%)	3 (3)	na	na
Thinning of the corpus callosum, n (%)	48 (49)	na	na
Dilation of the lateral ventricles, n (%)	39 (40)	na	na
Reduce white matter volume, n (%)	57 (58)	na	na
Increased extracerebral space, n (%)	28 (29)	na	na



	<b>Preterm Infants, n=98</b>	<b>Full-term Control Infants, n=104</b>	<b>P-value</b>
Deep gray matter signal abnormality, n (%)	6 (6)	na	na
Reduce deep gray matter volume, n (%)	8 (8)	na	na
Cerebellar signal abnormality, n (%)	16 (16)	na	na
Reduce cerebellar volume, n (%)	42 (43)	na	na
Brain injury category, n (%)			
Normal; Mild; Moderate	43 (44); 33 (34); 15 (15)	na	na

<sup>a</sup> not collected in five healthy full-term infants

<sup>b</sup> Brain abnormalities were scored using Kidokoro et al. classification.<sup>26</sup> The brain classification could not be used for seven preterm infants: their gestational age at MRI was higher than 42 weeks.

Table 2

Regional differences in cerebral blood flow.

	Absolute Cerebral Blood Flow (in mL/100g/min)				Relative Cerebral Blood Flow <sup>a</sup>			
	Preterm Infants (n=98)	Full-term Infants (n=104)	Mean difference <sup>b</sup>	Adjusted p-value <sup>b</sup>	Preterm Infants (n=98)	Full-term Infants (n=104)	Mean difference <sup>b</sup>	Adjusted p-value <sup>b</sup>
	Unadjusted mean ± SD	Unadjusted mean ± SD	Adjusted mean difference <sup>b</sup> [95% CI]	Adjusted p-value <sup>b</sup>	Unadjusted mean ± SD	Unadjusted mean ± SD	Adjusted mean difference <sup>b</sup> [95% CI]	Adjusted p-value <sup>b</sup>
Sensorimotor cortex	31.05 ± 5.4	20.26 ± 5.4	12.36 [5.99; 18.72]	<0.0001	1.6 ± 0.2	1.5 ± 0.3	0.03 [-0.17; 0.24]	1.00
Auditory cortex	23.05 ± 5.5	18.51 ± 3.6	6.1 [0.49; 11.71]	0.017	1.22 ± 0.2	1.41 ± 0.3	-0.23 [-0.42; -0.04]	0.0036
Visual cortex	23.73 ± 6.1	14.9 ± 3.8	10.38 [4.7; 16.04]	<0.0001	1.24 ± 0.2	1.13 ± 0.2	0.08 [-0.11; 0.27]	0.998
Superior medial prefrontal cortex	22.6 ± 4.8	16.76 ± 3.8	7.42 [1.88; 12.97]	0.0004	1.19 ± 0.2	1.26 ± 0.2	-0.03 [-0.29; 0.07]	1.0
Dorsolateral prefrontal cortex	17.32 ± 4.7	11.97 ± 3.2	6.91 [1.45; 12.38]	0.0013	0.9 ± 0.2	0.9 ± 0.2	-0.03 [-0.19; 0.14]	1.00
Anterior cingulate cortex	27.77 ± 5.7	22.39 ± 4.5	6.93 [1.2; 12.67]	0.0031	1.48 ± 0.3	1.7 ± 0.3	-0.26 [-0.48; -0.05]	0.0026
Posterior cingulate cortex	23.05 ± 6.4	16.44 ± 5	8.17 [2.32; 14]	0.0002	1.2 ± 0.2	1.23 ± 0.3	-0.06 [-0.26; 0.13]	0.999
Insula	31.69 ± 6.2	28.11 ± 5.2	5.14 [-0.69; 10.98]	0.171	1.68 ± 0.2	2.15 ± 0.4	-0.51 [-0.73; -0.28]	<0.0001
Lateral posterior parietal cortex	24.16 ± 6.3	16.72 ± 4.3	8.99 [3.23; 14.76]	<0.0001	1.26 ± 0.2	1.25 ± 0.2	-0.03 [-0.21; 0.14]	1.0
Basal ganglia	35.73 ± 8.7	23.62 ± 5.8	13.67 [7.3; 19.96]	<0.0001	1.86 ± 0.2	1.78 ± 0.3	0.05 [-0.16; 0.25]	1.0
Thalamus	38.5 ± 10.9	25.19 ± 7.1	14.87 [7.95; 21.79]	<0.0001	2.01 ± 0.3	1.89 ± 0.4	0.07 [-0.17; 0.31]	1.0
Brainstem	46.81 ± 13.8	32.23 ± 9.5	24.75 [17.53; 31.97]	<0.0001	2.46 ± 0.6	2.46 ± 0.7	-0.11 [-0.39; 0.34]	0.845

<sup>a</sup>Relative regional CBF was defined as the ratio of the absolute CBF of one ROI over the global CBF<sup>b</sup>The adjusted mean difference (preterm – full-term) and corresponding p-values are based on the mixed linear model in which group (preterm vs. full-term), brain regions, sex, gestational age at birth, day of life at MRI and the interaction between group and regions of interest are the fixed effects. The p-values are adjusted for multiple comparisons (Tukey-Kramer).

**Table 3**

Relationship between clinical risk factors and cerebral perfusion in the preterm cohort.

<b>Risk Factors</b>	<b>Preterm Infants (N=98)</b>	<b>Association with Cerebral Blood Flow<sup>a</sup> (<math>\beta</math>; [95% CI]; p-value)</b>
<b>Chorioamnionitis, n (%)</b>	20 (20)	NS
<b>Parenchymal brain injury, n (%)</b>	47 (48)	Global (-2.28; [-3.91; -0.64]; 0.007) Sensorimotor cortex (-3.74; [-7.36; -0.1]; 0.043) Auditory cortex (-3.73; [-5.9; -1.58]; <0.001) Visual cortex (-4.50; [-6.69; -2.28]; <0.001) Anterior cingulate cortex (-2.55; [-4.89; -0.22]; 0.032) Insula (-3.00; [-5.4; -0.56]; 0.016)
<b>Bronchopulmonary dysplasia (moderate/severe), n (%)</b>	47 (48)	NS
<b>Length of oxygen support, d, mean <math>\pm</math> SD</b>	75 (40)	NS
<b>Steroid treatment, n (%)</b>	41 (42)	NS
<b>Sepsis, n (%)</b>	15 (16)	NS
<b>Necrotizing enterocolitis, n (%)</b>	36 (37)	NS
<b>Pressor support, n (%)</b>	39 (40)	Visual cortex (-3.46; [-3.4; -0.01]; 0.0079) Insula (-3.29; [-5.89; -0.51]; 0.016)
<b>Patent ductus arteriosus ligation, n (%)</b>	25 (26)	NS

<sup>a</sup>Linear regression analysis included each individual clinical risk factor as well as sex, gestational age at birth and day of life at MRI.  $\beta$  is the regression coefficient associated with the risk factor in the model. NS = not significant.

**Table 4**

Predictors of global and regional cerebral perfusion in the preterm cohort (n=98)

Cerebral Blood Flow	Extended Model		Parenchymal Brain Injury		Cardiac Pressor Support		Gestational Age at Birth		Day of Life at MRI		Sex	
	R <sup>2</sup>	P	$\beta$ [95% CI]	P	$\beta$ [95% CI]	P	$\beta$ [95% CI]	P	$\beta$ [95% CI]	P	$\beta$ [95% CI]	P
Global	0.24	<0.0001	-2.13 [-3.77; -0.5]	0.01	-1.3 [-3.1;0.5]	0.15	1.11 [0.49;1.74]	0.0005	0.15 [0.08;0.24]	<0.0001	0.05 [-1.51;1.61]	0.95
SM	0.24	<0.0001	-3.35 [-6.97;0.27]	0.07	-3.54 [-7.56;0.47]	0.08	2.66 [1.28;4.05]	0.0002	0.38 [0.21;0.56]	<0.0001	-0.16 [-3.6;3.3]	0.93
AUD	0.18	0.002	-3.55 [-5.72; -1.39]	0.0016	-1.74 [-4.14;0.65]	0.15	0.7 [-0.12;1.53]	0.09	0.11 [0.01;0.22]	0.03	0.93 [-1.13;3.01]	0.37
VIS	0.35	<0.0001	-4.18 [-6.34; -2.01]	0.0002	-2.84 [-5.25; -0.44]	0.02	1.56 [0.73;2.38]	0.0003	0.27 [0.17-0.37]	<0.0001	-0.4 [-2.47;1.67]	0.7
smPFC	0.164	0.0049	-0.78 [-2.72;1.17]	0.43	-1.36 [-3.51;0.8]	0.22	1.19 [0.45;1.93]	0.002	0.18 [0.08;0.27]	0.003	-0.377 [-2.24;1.48]	0.68
dIPFC	0.26	<0.0001	-1.08 [-2.88;0.71]	0.23	-1.04 [3.04;0.95]	0.3	1.6 [0.9;2.28]	<0.0001	0.22 [0.14;0.3]	<0.0001	1.4 [-0.3;3.12]	0.11
ACC	0.12	0.03	-2.61 [-4.98; -0.25]	0.03	0.53 [-2.09;3.14]	0.69	1.15 [0.25;2.05]	0.01	0.14 [0.03;0.26]	0.01	0.54 [1.71;2.8]	0.63
PCC	0.11	0.056	na	na	na	na	na	na	na	na	na	na
Insula	0.24	0.0001	-2.67 [-5.1; -0.23]	0.029	-2.84 [-5.5; -0.19]	0.036	1.45 [0.53;2.36]	0.002	0.22 [0.1;0.33]	0.0003	-0.63 [-2.9;1.65]	0.58
IPPC	0.16	0.0057	-1.98 [-4.54;0.57]	0.126	-2.23 [-5.06;0.6]	0.121	1.33 [0.36;2.31]	0.0079	0.21 [0.08;0.33]	0.0011	1.326 [-1.12;3.77]	0.28
BG	0.19	0.0011	-1.88 [-5.33;1.58]	0.28	-2.52 [-6.21;1.45]	0.19	2.30 [0.96;3.6]	0.0008	0.35 [0.18;0.5]	<0.0001	-1.04 [-4.34;2.26]	0.53
THAL	0.05	0.07	na	na	na	na	na	na	na	na	na	na
Brainstem	0.02	0.83	na	na	na	na	na	na	na	na	na	na

ACC = anterior cingulate cortex; AUD = auditory cortex; BG = basal ganglia; dIPFC = dorsolateral prefrontal cortex; IPPC = lateral posterior parietal cortex; PCC = posterior cingulate cortex; SM = sensorimotor cortex; smPFC = superior medial prefrontal cortex; THAL = thalamus; VIS = visual cortex.